Molecular Vision 2021; 27:588-600 <http://www.molvis.org/molvis/v27/588>
Received 26 May 2021 | Accepted 20 September 2021 | Published 22 September 2021

A deep intronic substitution in *CNGB3* is one of the major causes of achromatopsia among Jewish patients

Hamzah Aweidah,[1] Manar Salameh,[1] Claudia Yahalom,[1] Anat Blumenfeld,[1] Michal Macarov,[1] Nicole Weisschuh,[2] Susanne Kohl,[2] Eyal Banin,[1] Dror Sharon[1]

(The last two authors contributed equally to this study.)

[1]*Department of Ophthalmology, Hadassah Medical Center, Faculty of Medicine, The Hebrew University of Jerusalem, Israel;* [2]*Institute for Ophthalmic Research, Centre for Ophthalmology, University of Tübingen, Tübingen, Germany*

Purpose: Although most (or even all) genes that can cause achromatopsia (ACHM) when mutated are known, some patients are still negative for mutations even after screening the coding sequence of all known genes. Our aim was to characterize the genetic and clinical aspects of a deep intronic (c.1663–1205G>A, IVS14–1205G>A) *CNGB3* variant.
Methods: Clinical evaluation included visual acuity testing, refractive error, a full clinical eye exam, full-field electroretinography (ffERG), color vision testing, and retinal imaging. Genetic analysis of *CNGB3* exons, as well as part of intron 14, was performed by Sanger sequencing of PCR products.
Results: Screening for the *CNGB3* c.1663–1205G>A variant revealed 17 patients belonging to 12 unrelated families who were either homozygous for this variant (7 cases, 5 families) or heterozygous in combination with another heterozygous known *CNGB3* mutation (10 cases, 7 families). All patients were diagnosed with cone-dominated disease, mainly complete ACHM. In all cases, the disease had an early, congenital onset. Visual acuity was markedly impaired, ranging between 0.07 and 0.32 on the Early Treatment Diabetic Retinopathy Study (ETDRS) scale (logarithm of the minimum angle of resolution [LogMAR] +1.18 to +0.50), with a mean visual acuity of 0.15 ETDRS (LogMAR +0.80). Additional typical signs of ACHM, including impaired color vision, light aversion, and nystagmus, were also noted in all patients. As is common in ACHM, fundus exams were largely unremarkable in most patients, with mild foveal RPE changes seen in some cases at older ages. ERG was available for 14 out of 17 patients, and in all of them—including infants from the age of 6 months—cone responses were nondetectable. In a few cases, rod involvement was also evident, with a mild reduction of amplitudes. Optical coherence tomography (OCT) imaging showed irregularity of the ellipsoid zone in the foveal area in some patients.
Conclusions: *CNGB3* is the most common cause of ACHM in patients of European descent; this is mainly due to a panethnic founder mutation, c.1148del. Here, we report on an intronic *CNGB3* variant that is more frequent than the c.1148del mutation in our cohort of Jewish patients. Among our ACHM cohort, 63.7% of patients had biallelic *CNGA3* mutations and 26.4% had biallelic *CNGB3* mutations. The phenotype of patients harboring the intronic mutation falls largely within the spectrum commonly seen in ACHM. Since gene therapy for *CNGB3* is currently under investigation, these patients might benefit from this promising therapy. Given that this variant is not detectable by current commonly used genetic testing platforms, these patients could easily be missed.

Achromatopsia (ACHM), also known as rod monochromacy, is a rare autosomal recessive congenital retinal disorder of cone signal transduction that affects an estimated 1 in 50,000 to 1 in 30,000 people worldwide [1,2]. However, it shows a much higher prevalence in specific areas, with 4% to 10% reported on Pingelap Island [3] and 1:5,000 reported in the Jerusalem area in Israel [4]. ACHM is characterized by poor visual acuity, pendular nystagmus, severe photophobia, a small central scotoma, eccentric fixation, and a reduced or complete loss of color discrimination [2,5].

Correspondence to: Dror Sharon, Department of Ophthalmology, Hadassah Medical Center, Faculty of Medicine, The Hebrew University of Jerusalem, Israel; Phone: (972) 2-6777112, FAX: (972) 2-6448917; email: dror.sharon1@mail.huji.ac.il

ACHM has been associated with mutations in one of the six following genes: *CNGA3* [6], *CNGB3* [7,8], *GNAT2* [9,10], *PDE6C* [11,12], *PDE6H* [13], and *ATF6* [14]. The first five genes encode functional components of the phototransduction cascade in cone photoreceptors, whereas *ATF6* encodes a key regulator of the unfolded protein response and cellular endoplasmic reticulum homeostasis.

The *CNGB3* gene encodes the beta subunit of the cyclic nucleotide-gated channel in cone photoreceptors, and mutations in this gene account for approximately 50%–80% of all ACHM cases of European descent [15,16]. Most mutations result in significantly altered or truncated polypeptides, including the prevalent founder mutation, c.1148delC, which accounts for ~66% of all *CNGB3* mutant alleles [2,15].

A recent detailed analysis of the *CNGB3* locus revealed that copy number variations (CNVs), as well as intronic variants, contribute to the disease prevalence. A detailed analysis of ACHM patients with a single heterozygous *CNGB3* mutation (and no other suspected mutation in the open reading frame) revealed nine CNVs encompassing 1 to 10 consecutive exons that could not be detected by routine Sanger sequencing of individual exons. These CNVs account for more than one-third of the missing mutations, showing that CNVs do not account for all missing alleles and leaving a considerable number of cases genetically unsolved [2].

A subsequent study using whole gene sequencing to identify possible intronic pathogenic variants revealed two pathogenic mutations—c.1663-2137C>T and c.1663–1205G>A. The latter is the eighth most frequent *CNGB3* pathogenic variant in the studied cohort [17]. In the current study, we focused on genetic and clinical analysis of the latter intronic variant, c.1663–1205G>A, which we found to be the most common *CNGB3* mutation in our cohort of Jewish patients with ACHM.

METHODS

Subjects: ACHM patients and family members were recruited in accordance with the principles of the Declaration of Helsinki. Following signing of written informed consent approved by the institutional review board of the Ethics Committee of the Hadassah Hebrew University Medical Center, blood samples were drawn for genetic analysis, and clinical characterization of phenotype was performed as detailed below.

Genetic analysis: Genomic DNA was extracted from peripheral blood samples using the Maxwell blood DNA purification kit (Promega Corporation, Madison, WI) following standard protocols. Subsequently, mutation analysis was performed by Sanger sequencing of PCR products using primers specific to each *CNGB3* (NM_019098.4; hg19) region (Table 1). Segregation analysis was performed on all families in which we were able to recruit additional family members.

Phenotype assessment: The clinical phenotype was characterized by a full ophthalmologic evaluation, including visual acuity testing, determination of refractive error, biomicroscopic examination of the anterior and posterior segments of the eye, and color vision testing using the Ishihara 38 plates and Farnsworth D-15 color vision tests. Best corrected visual acuity (BCVA) was documented for the last follow-up visit of the patient, and the average of both eyes was taken.

Most patients underwent full-field electroretinography testing (ffERG), some according to the International Society for Clinical Electrophysiology of Vision (ISCEV) standard [18] and some, at extremely young ages, under sedation using a short protocol, as detailed below. ffERG was recorded using corneal electrodes and a computerized system (UTAS 3,000, LKC, Gaithersburg, MD), as previously described [19]. Briefly, in the regular protocol, dark adaptation is performed for at least 30–40 min before recording dark-adapted followed by light-adapted responses. In the dark-adapted state, a rod response to a dim blue flash and a mixed cone-rod response to a white flash were acquired. Cone responses to 30 Hz flashes of white light were acquired under a background light of 21 cd/m^2. All responses were filtered at 0.3–500 Hz, and signal averaging was used. The average cone flicker and mixed rod cone responses of the two eyes were measured in each patient. Limits of normal are as follows: 30 Hz cone flicker: lower threshold of normal for amplitude, 60 μV; upper limit for implicit time, 33 msec; mixed cone-rod response: lower threshold of normal for b-wave amplitude, 400 μV; for a-wave, 100 μV; and rod response lower threshold of normal for amplitude, 200 μV.

A short protocol was performed in young children in which cones were tested first under light-adapted conditions (normal limits identical to regular protocol). After 2 min of dark adaptation, an attempt to record a rod response using a low-intensity blue stimulus was performed, followed by recording of a mixed cone-rod response to a standard white flash (200 μV < normal b-wave < 440 μV). In seven cases, when the subjects were old enough and able to cooperate, noninvasive retinal imaging by optical coherence tomography (OCT) was performed.

Statistical analysis: All tests were unpaired two-tailed *t* tests applied using GraphPad Prism and Microsoft Excel software, and a p value of 0.05 or less was considered statistically significant.

RESULTS

The inherited retinal disease (IRD) cohort at Hadassah Medical Center included 91 families (146 patients) diagnosed with ACHM. Prior to the identification of the *CNGB3* c.1663–1205G>A variant, the genetic cause of disease was known for 72 of the families: Fifty-eight had biallelic *CNGA3* mutations, 12 had biallelic *CNGB3* mutations, 1 had a digenic *CNGA3-CNGB3* mutations, and 1 had a biallelic homozygous *PDE6C* mutation. In addition, there were 19 families in which ACHM was suspected on clinical grounds, but a definite genetic diagnosis could not be made; of these, 2 families had a single heterozygous *CNGA3* mutation, 5 had a single heterozygous *CNGB3* mutation, and 12 did not have any mutation in known ACHM genes (Figure 1A).

Table 1. Primers used for polymerase chain reaction (PCR) for each gene region.

Gene	Location	Variant	Forward primer sequence (5'-3')	Reverse primer sequence (5'-3')
CNGB3	Exon 1	c.105_114delTCAGTCTCAG, p.(Gln36Lysfs*44)	ACTAGCTAAGGAGTTGCCTG	AATTAATGAAGATAAGCCCG
CNGB3	Exon 4	c.467C>T, p.(Ser156Phe)	AATCTGTATTCCACCAGCAC	CTCGTACCTTCCTGGATTAC
CNGB3	Exon 6	c.644–1G>C, p.(?)	CTCTGTAGAGGGTAGTGCC	TGCAGATAGCCAGTCAAAC
CNGB3	Exon 6	c.782A>G, p.(Asp261Gly)	CTCTGTAGAGGGTAGTGCC	TGCAGATAGCCAGTCAAAC
CNGB3	Exon 6	c.819delC, p.(Arg274Aspfs*5)	CTCTGTAGAGGGTAGTGCC	TGCAGATAGCCAGTCAAAC
CNGB3	Exon 9	c.1006G>T, p.(Glu336*)	GGAAACAGAGTTCTACTACATGC	TGACAGAGGCAGATAATAAGTC
CNGB3	Exon 10	c.1148delC, p.(Thr383Ilefs*13)	GCTGTATTTCAGAAACAACATGAATC	CATAAATTCATACAATGAAACAGAATG
CNGB3	Intron 14	c.1663–1205G>A, p.(?)	AGTCCCCTC CTAAGCCAAGT	TATGAGGCCCTTGGAACAC
CNGB3	Intron 14	c.1578+1G>A, p.(?)	TGTTATTGTAATAGGTATGGAGG	TCTAAAGAATAAGCCGTTGG
CNGB3	Exon 18	c.2328delC, p.(Arg777Glufs*52)	GTGGTGATCTTAGCCATTG	CTTTCGTTTCTCAAGGGTC

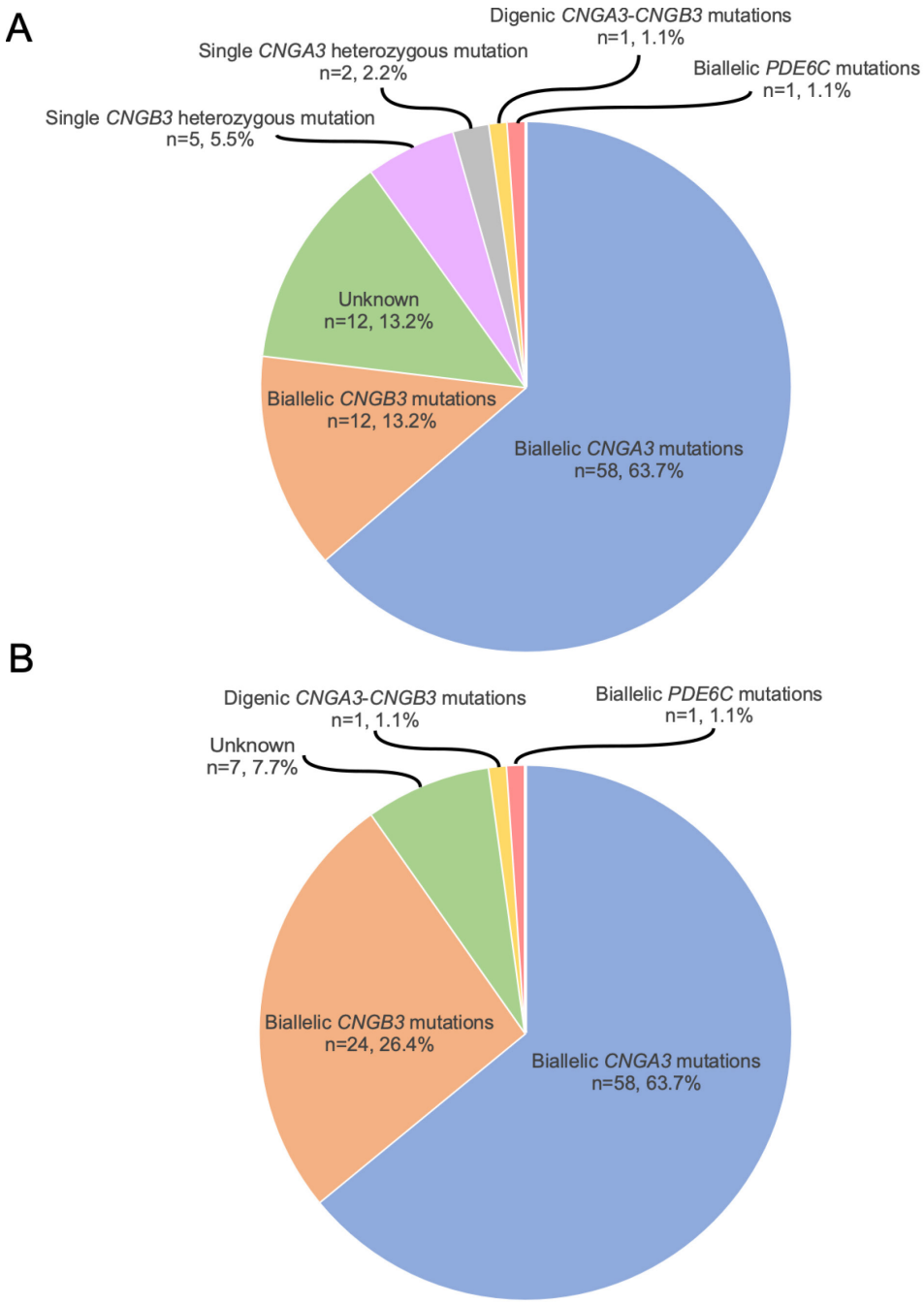

Figure 1. Distribution of achromatopsia causative genes before (**A**) and after (**B**) the identification of the *CNGB3* c.1663–1205G>A variant. *CNGB3* c.1663–1205G>A is one of the two common *CNGB3* mutations in our cohort. The letter "n" represents the number of families, and this number is followed by their proportion among all ACHM families in our cohort. Patients with one heterozygous mutation were considered unsolved, and they were added to the "unknown" group in panel **B**.

Aiming to examine whether the *CNGB3* c.1663–1205G>A intronic variant may explain some of the unsolved families, we screened the above-mentioned 19 nonsolved families for this intronic variant. Sanger sequencing revealed 12 families harboring the deep intronic variant: Seven patients from five families were homozygous for c.1663–1205G>A and 10 patients from seven families were heterozygous for c.1663–1205G>A *in trans* with a previously reported *CNGB3* mutation (including three patients from two families with c.1148delC, three patients from two families with

c.644–1G>C, three patients from two families with c.467C>T, and another index case with c.1578+1G>A). Moreover, we screened 36 additional index cases with cone-dominated retinal diseases other than ACHM (e.g., cone dystrophy and cone-rod dystrophy), but none of them was found to harbor the c.1663–1205G>A variant.

All index cases with c.1663–1205G>A were of Jewish origin of various ethnicities—mainly Iraqi Jews, Tunisian Jews, and Ashkenazi Jews (Table 2). All patients had a congenital onset of the retinal disease, characterized by impaired visual acuity, nystagmus, and photophobia. All were clinically diagnosed in childhood with a cone-related disease, with complete ACHM being the lead diagnosis, and in some of them, the differential diagnosis of cone-rod dystrophy was also suggested. Nine of the patients were males and eight were females, with a mean age of first presentation to our clinic and a diagnosis of 7.35 years (ranging from 6 months to 28 years).

Visual acuity for all patients with ACHM ranged between 0.01 and 0.32 on the Early Treatment Diabetic Retinopathy Study (ETDRS) scale (logarithm of the minimum angle of resolution [LogMAR] +2.00 to +0.50) with a mean ± standard deviation (SD) visual acuity of 0.12 ± 0.068 ETDRS (LogMAR +0.92 ± 1.22; Table 2 and Table 3). Refractive error ranged between −7.00 diopter (D) and +6.50 D: Three patients manifested high myopia (mean spherical equivalent [SE] of both eyes ≥ −6.00 D), five had hypermetropia ≥ +4.00 D, and the remaining 27 of the 35 subjects manifested refractive errors between these values, with a mean spherical equivalent of −0.43 ± 3.2 D (Table 2 and Table 3). For those who were old enough to perform color vision tests, all had severe color vision deficiency as tested using the Ishihara and Farnsworth D-15 tests.

Disease expression in c.1663–1205G>A homozygotes: All seven c.1663–1205G>A homozygous patients showed nystagmus, photophobia, nondetectable cone ERG responses, and impaired color discrimination. Data regarding visual acuity are available for six of the patients, four of whom showed severely reduced visual acuity (less than or equal to 0.13 ETDRS, LogMAR +0.88). Visual acuity ranged from 0.07 to 0.32 ETDRS (LogMAR +1.18 to +0.50), and refractive errors ranged from high myopia (−6.94 D) to high hypermetropia (+5.75 D), with two patients manifesting high myopia and one high hypermetropia (Table 2).

Funduscopic findings were minimal, spanning from a normal appearance to mild foveal pigmentary or subtle atrophic changes. Color vision testing was abnormal in all patients who were old enough to undergo this evaluation. On the Ishihara 38-plate color vision test, results ranged from inability to identify even the demonstration panel (this is not dependent on color discrimination but rather reflects poor visual acuity), identification of the demonstration panel alone, and in a few cases, correct identification of a small number of plates. On the Farnsworth D-15 test, multiple errors were observed in all patients, usually manifesting as a mixture of all possible axes of confusion, including scotopic lines. ffERG testing was available in five of the seven homozygous patients. In all cases, cone responses were nondetectable, whereas rod-derived responses were essentially normal (Table 2).

Disease expression in compound heterozygotes for c.1663–1205G>A: We identified 10 patients who were compound heterozygotes for c.1663–1205G>A and another known *CNGB3* mutation in the coding regions. All 10 patients showed severely reduced visual acuity, as well as nystagmus, nondetectable cone ERG responses, and impaired color discrimination. Visual acuity ranged from 0.10 to 0.20 ETDRS (LogMAR +1.00 to +0.70). One patient manifested high hypermetropia (+6.40 D), one had high myopia (−6.65 D), five had mild to moderate myopia, and three had hypermetropia (Table 2). Funduscopic findings were similar to those of the homozygous group, with most patients presenting a normal fundus appearance. ffERG was performed at our center in 7 of the 10 patients (a short protocol under sedation was used in three patients because of their extremely young age). Three others were tested in a different hospital. In all 10 compound heterozygous patients, cone responses were nondetectable, whereas rod-derived responses were either normal or subnormal (Table 2). Segregation analysis was performed in five out of seven families with two heterozygous variants. In summary, the phenotype of patients homozygous for the c.1663–1205G>A intronic variant did not differ from those in whom this mutation was in the compound heterozygous state together with another pathogenic *CNGB3* mutation.

ACHM in patients with CNGB3 mutations other than c.1663–1205G>A: Our *CNGB3* cohort includes an additional 18 patients from 12 different families in whom the c.1663–1205G>A mutation is not present, and we sought to see whether they might manifest a different phenotype. Eight of the patients (who belong to five unrelated families) were homozygotes for the most common *CNGB3* mutation worldwide, c.1148delC. Two patients from one family were homozygotes for the canonical splice-site variant c.644–1G>C, two patients from one family were homozygotes for the missense variant c.782A>G (p.D261G), and one patient from another family was a homozygote for the p.E336* nonsense mutation. The remaining five patients had compound heterozygotes for different exonic *CNGB3* mutations (Table 3).

Patient ID (Age at diagnosis, years)	Origin	Consanguinity	Genotype	Visual Acuity‡ (Age at visual acuity test, years)	Spherical Equivalent (SE)§	Full Field ERG amplitudes (μV)§§			
						Age at ffERG test (years)	LA 30Hz Cone Flicker (IT)	DA Mixed Rod-Cone (Average)	Rod response (b wave)
MOL1848–1 (06)	Mixed Jewish[b] (Iraq/Morocco, Iraq/Turkey)	None	c.1148delC;1663-1205G>A	0.16 (12)	−1.50	6	ND	a: 68 b: 215	198
MOL1894–1 (13)	Mixed Jewish[b] (Egypt/ Egypt, Iraq)	None	c.467C>T;1663–1205G>A	0.12 (41)	−6.65	NA	ND	NA[a]	NA[a]
MOL1894–2 (01)	Mixed Jewish[b] (Egypt / Egypt, Iraq)	None	c.467C>T;1663–1205G>A	0.17 (46)	+2.50	NA	ND	NA[a]	NA[a]
MOL1954–1 (02)	Mixed Jewish[b] (Yemen, Bulgaria / Ukraine)	None	c.[1578+1G>A];[1663-1205G>A]	CSM (2)	−0.75	2	ND	Mild reduction*	Reduced*

‡Best corrected visual acuity is presented as an average of the two eyes, in decimal values. To provide numerical values for low visual acuity, the following conversions were made: NLP (no light perception)=0; LP (light perception)=0.0001; HM (hand movement)=0.001; FC (finger counting)=0.01.§Average of spherical equivalent of both eyes, in diopters. ND- Non-detectable. NA- Not available. CSM- Central, steady, and maintained. [a] Done in different hospital. [b] Mixed Jewish (Father origin/ Mother origin). §§ Full field ERG testing performed according to ISCEV standard; average of the values recorded in the two eyes are shown for each of the main stimulus conditions. Limits of normal are as follows: 30Hz Cone Flicker: lower threshold of normal for amplitude-60μV; upper limit for implicit time- 33msec; Mixed cone-rod response- lower threshold of normal for b wave amplitude- 400μV; for a- wave- 100μV; Rod response- lower threshold of normal for amplitude- 200μV. * Short protocol ffERG: in young patients, a short protocol was performed under sedation. Cones are tested first under light-adapted conditions with the same reference values as above. After two minutes of dark-adaptation, a mixed cone-rod response to a standard flash is recorded (b- wave amplitude >200 μV). Rod responses cannot be accurately quantified under these conditions.

Molecular Vision 2021; 27:588-600 <http://www.molvis.org/molvis/v27/588>

Molecular Vision 2021; 27:588-600 <http://www.molvis.org/molvis/v27/588>

Table 3. Patients with other *CNGB3* mutations causing achromatopsia.

Patient ID (age at ERG testing, years)	Origin	Consanguinity	Genotype	Visual Acuity‡ (Age at visual acuity test, years)	Spherical Equivalent (SE)§	Full Field ERG amplitudes (μV)			
						Age at ffERG test (years)	LA 30Hz Cone Flicker (IT)	DA Mixed Rod-Cone (Average)	Rod response (b wave)
MOL0686–1 (10)	Moroccan Jewish	Yes (1:2)	c.[1148delC];[1148delC]	0.01 (41)	NA	41	ND	a: 142 b: 243	184
MOL0831–4 (0.5)	Tunisian Jewish	Yes (2:2)	c.[1148delC];[1148delC]	0.10 (31)	+4.25	31	ND	a: 126 b: 258	138
MOL0831–5 (12)	Tunisian Jewish	Yes (2:2)	c.[1148delC];[1148delC]	0.10 (20)	+0.25	20	ND	a: 182 b: 298	247.50
MOL1136–1 (01)	Moroccan Jewish	None	c.[1148delC];[1148delC]	0.08 (2)	+4.00	2	NA	Lower normal*	NA*
MOL1391–1 (04)	Moroccan Jewish	None	c.[1148delC];[1148delC]	NA	+2.56	4	ND	Moderate reduction*	Normal*
MOL1391–2 (03)	Moroccan Jewish	None	c.[1148delC];[1148delC]	NA	+1.25	3	ND	Reduced*	Normal*
RD175–1 (04)	Mixed Jewish (Algeria, Morocco)	None	c.[1148delC];[1148delC]	0.16 (11)	−1.19	NA[a]	NA[a]	NA[a]	NA[a]
RD175–2 (08)	Mixed Jewish (Algeria, Morocco)	None	c.[1148delC];[1148delC]	0.20 (15)	−1.38	NA[a]	NA[a]	NA[a]	NA[a]
MOL0012–1 (12)	Ashkenazi Jews	None	c.[644–1G>C];[644–1G>C]	0.01 (40)	+1.50	40	ND	a: 134.5 b: 285.5	304.50
MOL0012–3 (01)	Ashkenazi Jews	None	c.[644–1G>C];[644–1G>C]	0.10 (20)	NA	20	ND	a: 104 b: 326	340.50
MOL0360–1 (0.5)	Bedouin	Yes (2:2)	c.[782A>G];[782A>G]	NA	+1.58	7	Severe reduction	Reduced*	NA*
MOL0360–2 (05)	Bedouin	Yes (2:2)	c.[782A>G];[782A>G]	0.01 (5)	−1.25	5	ND	Normal Rods*	NA*
MOL1173–1 (03)	Georgian Jews	None	c.[1006G>T];[1006G>T]	NA	+1.88	3	Severe reduction	Moderate to severe reduction*	NA*
MOL0663–1 (13)	Georgian Jews	None	c.[1006G>T];[2328delC]	0.10 (13)	+2.00	13	ND	a: 76.5 b: 236	174
MOL0663–2 (16)	Georgian Jews	None	c.[1006G>T];[2328delC]	0.10 (18)	−0.88	18	ND	a: 60.5 b: 283	189.5

Patient ID (age at ERG testing, years)	Origin	Consan-guinity	Genotype	Visual Acuity‡ (Age at visual acuity test, years)	Spherical Equiva-lent (SE)§	Full Field ERG amplitudes (μV)			
						Age at ffERG test (years)	LA 30Hz Cone Flicker (IT)	DA Mixed Rod-Cone (Average)	Rod response (b wave)
MOL1190–1 (20)	Ashkenazi Jews	None	c.[1148delC];[c.819delC]	0.14 (31)	NA	NA	NA[a]	NA[a]	NA[a]
MOL0344–1 (02)	Ashkenazi Jews	None	c.[467C>T];[644–1G>C]	0.10 (28)	+1.80	28	ND	a: 150 b: 200	NA**
MOL1535–1 (0.5)	Arab Christian	Yes (5:5)	c.[105_114delTCAGTCTCAG]; [105_114delTCAGTCTCAG]	0.08 (7)	+5.30	1.5	ND	Mild reduction*	NA*

‡Best corrected visual acuity is presented as an average of the two eyes, in decimal values. To provide numerical values for low VA, the following conversions were made: NLP (no light perception)=0; LP (light perception)=0.0001; HM (hand movement)=0.001; FC (finger counting)=0.01.§Average of spherical equivalent of both eyes, in diopters. ND-Non-detectable. NA- Not available. ** Technical difficulties. [a] Done in different hospital. §§ Full field ERG testing performed according to ISCEV standard; average of the values recorded in the two eyes are shown for each of the main stimulus conditions. Limits of normal are as follows: 30Hz Cone Flicker: lower threshold of normal for amplitude-60μV; upper limit for implicit time- 33msec; Mixed cone-rod response- lower threshold of normal for b wave amplitude- 400μV; for a- wave- 100μV; Rod response- lower threshold of normal for amplitude- 200μV. * Short protocol ffERG: in young patients, a short protocol was performed under sedation. Cones are tested first under light-adapted conditions with the same reference values as above. After two minutes of dark-adaptation, a mixed cone-rod response to a standard flash is recorded (b- wave amplitude >200 μV). Rod responses cannot be accurately quantified under these conditions.

Molecular Vision ####; ###:588-600 <http://www.molvis.org/molvis/v/####/###>

The patients in this group were divided equally between males and females and were again characterized by impaired visual acuity, nystagmus, and photophobia. All were clinically diagnosed with a congenital onset cone-related disease, with complete ACHM being the lead diagnosis. The mean age at first presentation to our clinic and diagnosis was 6.4 years (ranging from 5 months to 20 years).

Visual acuity in this group ranged between 0.01 and 0.20 ETDRS (LogMAR +2.00 to +0.70), with a mean visual acuity of 0.09 ± 0.05 ETDRS (LogMAR +1.04 ± 1.3). Most subjects had a mild hypermetropic refractive error (n = 8, mean SE ranging from +0.25 to +2.56 D); three other patients had higher hypermetropia ranging from +4.00 to +5.31 D, and four subjects had mild myopia ranging from −0.88 to −1.37 D (refractive error was not available in three patients). All subjects had severe color vision deficiency as tested using the Ishihara and Farnsworth D-15 tests (Table 3).

In comparing clinical characteristics of *CNGB3* ACHM patients who harbor at least one intronic c.1663–1205G>A mutation to patients who do not carry this variant, the differences in most parameters were not statistically significant (Table 4). In one parameter only, BCVA, patients with the intronic mutation were found to have slightly better visual acuity: The mean visual acuity in patients with the intronic mutation (homozygous and heterozygous; n = 17) was 0.15 ± 0.07, whereas in patients with other biallelic *CNGB3* mutations (n = 18), the mean BCVA was 0.092 ± 0.053 (p = 0.0215).

DISCUSSION

Disease-causing mutations are usually identified within or in close proximity to the coding exonic regions of the causative gene(s). However, recent accumulating data show that mutations in noncoding regions, and especially deep intronic single nucleotide alterations, can also be a relatively common cause of disease. The large size of introns in the human genome, the high number of nonpathogenic variants within introns, and the abundance of repetitive elements make the identification of deep intronic single nucleotide mutations an extremely challenging task. An important example of such a mutation is c.2991+1655A>G in *CEP290*, which creates a strong donor splice site, resulting in the inclusion of a cryptic exon in the *CEP290* mRNA [20]. Such deep intronic mutations are likely to be present in almost every gene associated with an inherited human phenotype. Recently, a large cohort of 1,100 unrelated ACHM patients was studied, and 5% were found to harbor a single *CNGB3* heterozygous mutation, raising the possibility that deep intronic mutations may account for the missing mutated alleles [2,17]. Sequencing the entire *CNGB3* locus in 33 of these cases revealed two novel deep intronic pathogenic variants—c.1663-2137C>T and c.1663–1205G>A—the latter being the eighth most frequent *CNGB3* variant in the studied cohort [17]. A splicing assay in HEK293T cells revealed the inclusion of a pseudoexon of 34 nucleotides between exons 14 and 15 in 68% of the transcripts in these in vitro assays. Therefore, the authors

Table 4. Comparison of different characteristics between the c.1663-1205G>A deep intronic *CNGB3* variant and the other *CNGB3* mutations causing achromatopsia.

Characteristics	Patients with *CNGB3* c.1663-1205G>A (Mean±SD; Mean±95% CI)	Patients with other *CNGB3* mutations (Mean±SD; Mean±95% CI)	*P* value
Age at diagnosis (years)	7.35±7.93; 7.35±3.77	6.42±5.86; 6.42±2.71	p=0.70
Age at first ERG (years)	7.53±8.26; 7.53±4.18	7.58±7.99; 7.58±3.69	p=0.99
Age at the last included ERG (years)	12.69±9.69; 12.69±5.27	15.77±13.43; 15.77±6.80	p=0.51
Age at last included visual acuity (years)	18.75±12.21; 18.75±5.99	20.14±12.02; 20.14±6.30	p=0.76
Current age (years)	22.82±12.45; 22.82±5.92	27.22±17.03; 27.22±7.87	p=0.41
Sex	9 Males, 8 Females	9 Males, 9 Females	
Visual acuity[‡]	0.15±0.07; 0.15±0.034	0.092±0.053; 0.092±0.028	**p=0.0215**
Mean Spherical equivalent[§]	−0.58±3.83; −0.58±1.88	+1.45±2.00; +1.45±1.01	p=0.088
ffERG Cone- Rod response a-wave (μV)[§]	134.94±50.15; 134.94±34.75	121.94±37.30; 121.94±25.85	p=0.59
ffERG Cone- Rod response b-wave (μV)[§]	258.81±51.52; 258.81±35.70	266.19±37.32; 266.19±25.86	p=0.76
ffERG Rod response (b-wave; μV)[§]	221.36±50.85; 221.36±37.67	225.43±68.95; 225.43±51.08	p=0.91

Table 5. The most common ACHM-causing variants in our cohort of patients.

ACHM-causing gene	c. Variant	p. Variant	Number of families	Number of patients	Number of alleles
CNGA3	c.1585G>A	p.V529M	17	41	76
CNGA3	c.940_942delATC	p.I314del	13	33	61
CNGA3	c.1669G>A	p.G557R	12	20	29
CNGB3	c.1663–1205G>A	IVS14–1205G>A	12	17	24
CNGB3	c.1148delC	p.T383Ifs*12	8	12	20

concluded that the c.1663–1205G>A variant may represent a mild allele that might be associated with reduced levels of the wild-type *CNGB3* transcript and protein. Since one of the patients reported to be a compound heterozygote for this mutation was of Jewish ancestry, the focus of the current study was to examine the frequency of the c.1663–1205G>A variant in Jewish patients with cone-dominated diseases and to assess the disease severity associated with this variant. In the current study, we identified 17 patients belonging to 12 families who harbored c.1663–1205G>A either homozygously or in a compound heterozygous state (the phase could be verified in five out of the seven families for which samples of relatives were available), and therefore, it is one of the two most common *CNGB3* mutations in our cohort (34.4% of all *CNGB3* alleles identified in ACHM patients in our cohort; Figure 2). The second most common mutation was c.1148delC, identified in 12 patients from eight unrelated Jewish families (eight patients from five families were homozygous and four patients from three families were compound heterozygous). Identifying the c.1663–1205G>A mutation reduced the unknown genetic cause in our cohort from 19 families with suspected ACHM to 7 families and helped us to identify the second causative mutation in another group of patients (Figure 1B). The five most common ACHM mutations in our cohort are shown in Table 5. The three most common mutations are founder mutations in *CNGA3*.

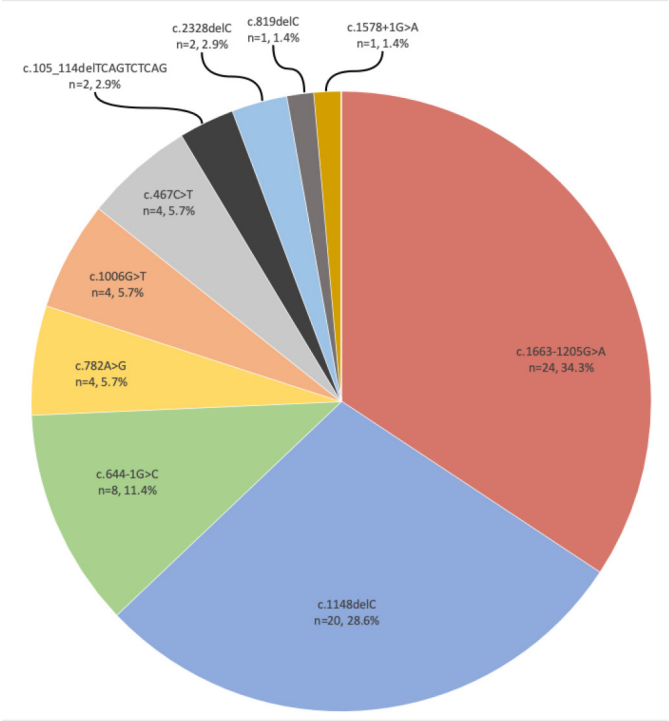

Figure 2. The distribution of *CNGB3* causative variants in our cohort. The *CNGB3* c.1663–1205G>A variant is the most common (34.4% out of all *CNGB3* pathogenic alleles), whereas the panethnic mutation, c.1148del, has been identified in 28.6% of alleles. The letter "n" represents the number of alleles identified in affected individuals, and this number is followed by their proportion among *CNGB3* mutated alleles.

Since c.1663–1205G>A was found to partially affect *CNGB3* splicing in minigene assays, it has been proposed that it may act as a mild allele leading to an incomplete ACHM phenotype in homozygous individuals and possibly in compound heterozygotes as well [17]. However, our clinical analysis does not support this hypothesis, and there was no statistically significant difference in most visual function parameters of patients harboring c.1663–1205G>A compared to other ACHM patients. The only exception was visual acuity, which indeed was better (average of 0.15) in patients harboring c.1663-1205G>A compared with other *CNGB3* patients (average of 0.09). This difference might stem from the production of normal transcripts by the c.1663-1205G>A-bearing allele in cone photoreceptor cells.

Because of their focus on the protein coding regions, routine diagnostic tests do not usually identify pathogenic deep intronic variants. However, common deep intronic variants are often included in commercial genetic testing panels, but the c.1663–1205G>A is currently not included in most panels, and given its frequency as reported here, we recommend adding it to those panels. Therefore, the use of novel approaches, such as whole genome sequencing, has facilitated the scanning of an entire gene and uncovered deep-intronic splice mutations in multiple IRD genes. Such mutations—and mainly founder mutations like the one reported here—should be added to gene and mutation panels to ensure that every mutation, disregarding its location, is identified and reported to the individuals who carry them.

ACKNOWLEDGMENTS

The authors thank all patients and referring clinicians for their participation in the study. This study was supported by the Foundation Fighting Blindness USA (grant BR-GE-0214–0639 to DS and EB), the Yedidut Research grant (to EB), the Israeli Ministry of Health (grant 3–12583 to DS and EB), and by the Israel Science Foundation (grant No. 1778/20 to DS and EB), within the Israel Precision Medicine Partnership program. Dr. Sharon (dror.sharon1@mail.huji.ac.il) and Dr. Banin (banine@mail.huji.ac.il) are co-corresponding authors for this paper.

REFERENCES

1. Michaelides M, Hunt DM, Moore AT. The cone dysfunction syndromes. Br J Ophthalmol 2004; 88:291-7. [PMID: 14736794].

2. Mayer AK, Van Cauwenbergh C, Rother C, Baumann B, Reuter P, De Baere E, Wissinger B, Kohl S. CNGB3 mutation spectrum including copy number variations in 552 achromatopsia patients. Hum Mutat 2017; 38:1579-91. [PMID: 28795510].

3. Brody JA, Hussels I, Brink E, Guam A, Torres J. Hereditary blindness among Pingelapese people of Eastern Caroline Islands. Lancet 1970; 1:1253-7. [PMID: 4192495].

4. Zelinger L, Cideciyan AV, Kohl S, Schwartz SB, Rosenmann A, Eli D, Sumaroka A, Roman AJ, Luo X, Brown C, Rosin B, Blumenfeld A, Wissinger B, Jacobson SG, Banin E, Sharon D. Genetics and disease expression in the CNGA3 form of achromatopsia: Steps on the path to gene therapy. Ophthalmology 2015; 122:997-1007. [PMID: 25616768].

5. Langlo CS, Erker LR, Parker M, Patterson EJ, Higgins BP, Summerfelt P, Razeen MM, Collison FT, Fishman GA, Kay CN, Zhang J, Weleber RG, Yang P, Pennesi ME, Lam BL, Chulay JD, Dubra A, Hauswirth WW, Wilson DJ, Carroll J. Repeatability and longitudinal assessment of foveal cone structure in CNGB3 -Associated achromatopsia. Retina 2017; 37:1956-66. [PMID: 28145975].

6. Kohl S, Marx T, Giddings I, Jägle H, Jacobson SG, Apfelstedt-Sylla E, Zrenner E, Sharpe LT, Wissinger B. Total colourblindness is caused by mutations in the gene encoding the α-subunit of the cone photoreceptor cGMP-gated cation channel. Nat Genet 1998; 19:257-9. [PMID: 9662398].

7. Sundin OH, Yang JM, Li Y, Zhu D, Hurd JN, Mitchell TN, Silva ED, Maumenee IH. Genetic basis of total colourblindness among the Pingelapese islanders. Nat Genet 2000; 25:289-93. [PMID: 10888875].

8. Kohl S. Mutations in the CNGB3 gene encoding the beta-subunit of the cone photoreceptor cGMP-gated channel are responsible for achromatopsia (ACHM3) linked to chromosome 8q21. Hum Mol Genet 2000; 9:2107-16. [PMID: 10958649].

9. Kohl S, Baumann B, Rosenberg T, Kellner U, Lorenz B, Vadalà M, Jacobson SG, Wissinger B. Mutations in the cone photoreceptor G-protein α-subunit gene GNAT2 in patients with achromatopsia. Am J Hum Genet 2002; 71:422-5. [PMID: 12077706].

10. Aligianis IA, Forshew T, Johnson S, Michaelides M, Johnson CA, Trembath RC, Hunt DM, Moore AT, Maher ER. Mapping of a novel locus for achromatopsia (ACHM4) to 1p and identification of a germline mutation in the α subunit of cone transducin (GNAT2). J Med Genet 2002; 39:656-660. [PMID: 12205108].

11. Thiadens AAHJ, den Hollander AI, Roosing S, Nabuurs SB, Zekveld-Vroon RC, Collin RWJ, De Baere E, Koenekoop RK, van Schooneveld MJ, Strom TM, van Lith-Verhoeven JJC, Lotery AJ, van Moll-Ramirez N, Leroy BP, van den Born LI, Hoyng CB, Cremers FPM, Klaver CCW. Homozygosity Mapping Reveals PDE6C Mutations in Patients with Early-Onset Cone Photoreceptor Disorders. Am J Hum Genet 2009; 85:240-7. [PMID: 19615668].

12. Chang B, Grau T, Dangel S, Hurd R, Jurklies B, Cumhur Sener E, Andreasson S, Dollfus H, Baumann B, Bolz S, Artemyev N, Kohl S, Heckenlively J, Wissinger B. A homologous

genetic basis of the murine cpfl1 mutant and human achromatopsia linked to mutations in the PDE6C gene. Proc Natl Acad Sci USA 2009; 106:19581-6. [PMID: 19887631].

13. Kohl S, Coppieters F, Meire F, Schaich S, Roosing S, Brennenstuhl C, Bolz S. Van genderen MM, Riemslag FCC, Lukowski R, Den hollander AI, Cremers FPM, De baere E, Hoyng CB, Wissinger B. A nonsense mutation in PDE6H causes autosomal-recessive incomplete achromatopsia. Am J Hum Genet 2012; 91:527-32. [PMID: 22901948].

14. Kohl S, Zobor D, Chiang WC, Weisschuh N, Staller J, Menendez IG, Chang S, Beck SC, Garrido MG, Sothilingam V, Seeliger MW, Stanzial F, Benedicenti F, Inzana F, Héon E, Vincent A, Beis J, Strom TM, Rudolph G, Roosing S, Hollander AID, Cremers FPM, Lopez I, Ren H, Moore AT, Webster AR, Michaelides M, Koenekoop RK, Zrenner E, Kaufman RJ, Tsang SH, Wissinger B, Lin JH. Mutations in the unfolded protein response regulator ATF6 cause the cone dysfunction disorder achromatopsia. Nat Genet 2015; 47:757-65. [PMID: 26029869].

15. Kohl S, Varsanyi B, Antunes GA, Baumann B, Hoyng CB, Jägle H, Rosenberg T, Kellner U, Lorenz B, Salati R, Jurklies B, Farkas A, Andreasson S, Weleber RG, Jacobson SG, Rudolph G, Castellan C, Dollfus H, Legius E, Anastasi M, Bitoun P, Lev D, Sieving PA, Munier FL, Zrenner E, Sharpe LT, Cremers FPM, Wissinger B. CNGB3 mutations account for 50% of all cases with autosomal recessive achromatopsia. Eur J Hum Genet 2005; 13:302-8. [PMID: 15657609].

16. Thiadens AAHJ, Slingerland NWR, Roosing S, van Schooneveld MJ, van Lith-Verhoeven JJC, van Moll-Ramirez N, van den Born LI, Hoyng CB, Cremers FPM, Klaver CCW. Genetic Etiology and Clinical Consequences of Complete and Incomplete Achromatopsia. Ophthalmology 2009; 116:1984-1989.e1. [PMID: 19592100].

17. Weisschuh N, Sturm M, Baumann B, Audo I, Ayuso C, Bocquet B, Branham K, Brooks BP, Catalá-Mora J, Giorda R, Heckenlively JR, Hufnagel RB, Jacobson SG, Kellner U, Kitsiou-Tzeli S, Matet A, Martorell Sampol L, Meunier I, Rudolph G, Sharon D, Stingl K, Streubel B, Varsányi B, Wissinger B, Kohl S. Deep-intronic variants in CNGB3 cause achromatopsia by pseudoexon activation. Hum Mutat 2020; 41:255-64. [PMID: 31544997].

18. McCulloch DL, Marmor MF, Brigell MG, Hamilton R, Holder GE, Tzekov R, Bach M. ISCEV Standard for full-field clinical electroretinography (2015 update). Doc Ophthalmol 2015; 130:1-12. [PMID: 25502644].

19. Beit-Ya'acov A, Mizrahi-Meissonnier L, Obolensky A, Landau C, Blumenfeld A, Rosenmann A, Banin E, Sharon D. Homozygosity for a novel ABCA4 founder splicing mutation is associated with progressive and severe Stargardt-like disease. Invest Ophthalmol Vis Sci 2007; 48:4308-14. [PMID: 17724221].

20. den Hollander AI, Koenekoop RK, Yzer S, Lopez I, Arends ML, Voesenek KEJ, Zonneveld MN, Strom TM, Meitinger T, Brunner HG, Hoyng CB, Van Den Born LI, Rohrschneider K, Cremers FPM. Mutations in the CEP290 (NPHP6) gene are a frequent cause of leber congenital amaurosis. Am J Hum Genet 2006; 79:556-61. [PMID: 16909394].

Articles are provided courtesy of Emory University and the Zhongshan Ophthalmic Center, Sun Yat-sen University, P.R. China. The print version of this article was created on 22 September 2021. This reflects all typographical corrections and errata to the article through that date. Details of any changes may be found in the online version of the article.